APL Materials

Flexible ITO-free organic solar cells applying aqueous solution-processed V_2O_5 hole transport layer: An outdoor stability study

Cite as: APL Mater. 4, 026104 (2016); https://doi.org/10.1063/1.4942638
Submitted: 05 December 2015 • Accepted: 04 February 2016 • Published Online: 24 February 2016

F. Anderson S. Lima, Michail J. Beliatis, Bérenger Roth, et al.

Flexible ITO-free organic solar cells applying aqueous solution-processed V_2O_5 hole transport layer: An outdoor stability study

F. Anderson S. Lima,[1,2,3] Michail J. Beliatis,[4] Bérenger Roth,[4] Thomas R. Andersen,[4] Andressa Bortoti,[2,3,5] Yegraf Reyna,[2,3] Eryza Castro,[5] Igor F. Vasconcelos,[1] Suren A. Gevorgyan,[4] Frederik C. Krebs,[4] and Mónica Lira-Cantu[2,3,6]

[1]*Departamento de Engenharia Metalúrgica e de Materiais, Universidade Federal do Ceará, Campus do Pici - Bloco 729, Fortaleza, CE 60440-554, Brazil*
[2]*Catalan Institute of Nanoscience and Nanotechnology (ICN2), Campus UAB, Bellaterra, 08193 Barcelona, Spain*
[3]*Barcelona Institute of Science and Technology (BIST), Campus UAB, Bellaterra, 08193 Barcelona, Spain*
[4]*Department of Energy Conversion and Storage, Technical University of Denmark, Frederiksborgvej 399, DK-4000 Roskilde, Denmark*
[5]*Departamento de Química, Universidade Estadual do Centro-Oeste – UNICENTRO, Campus CEDETEG, Guarapuava, PR, Brazil*
[6]*Consejo Superior de Investigaciones Científicas (CSIC), Campus UAB, Bellaterra, E-08193 Barcelona, Spain*

(Received 5 December 2015; accepted 4 February 2016; published online 24 February 2016)

Solution processable semiconductor oxides have opened a new paradigm for the enhancement of the lifetime of thin film solar cells. Their fabrication by low-cost and environmentally friendly solution-processable methods makes them ideal barrier (hole and electron) transport layers. In this work, we fabricate flexible ITO-free organic solar cells (OPV) by printing methods applying an aqueous solution-processed V_2O_5 as the hole transport layer (HTL) and compared them to devices applying PEDOT:PSS. The transparent conducting electrode was PET/Ag/PEDOT/ZnO, and the OPV configuration was PET/Ag/PEDOT/ZnO/P3HT:PC_{60}BM/HTL/Ag. Outdoor stability analyses carried out for more than 900 h revealed higher stability for devices fabricated with the aqueous solution-processed V_2O_5. [http://dx.doi.org/10.1063/1.4942638]

Over the last few years, the use of transition metal oxides (TMOs) with a large work function (WF) like NiO,[1] MoO_3,[2,3] WO_3,[4] or V_2O_5,[5] among others, has materialized as a viable option for their application as hole-transport layer in stable organic solar cells (OPV). The development of solution processing TMOs has also been successfully applied in perovskite solar cells.[6–8] The resulting oxide thin films have shown properties comparable to those grown by vacuum-processed resulting in devices with comparable or enhanced power conversion efficiencies (PCEs) and lifetime. Such is the case of NiO,[9] MoO_3,[10,11] CuO,[12] or V_2O_5.[13,14] For V_2O_5, one of its most widespread fabrication methods is the application of sol-gels made from vanadium (V) oxitriisopropoxide (V_2O_5–i)[14–18] or $(NH_4)_3VO_4$.[19,20,25] These precursors when used for the fabrication of flexible organic solar cells must be annealed at temperatures not exceeding 150 °C leaving behind organic residues that affect the OPV properties. In this work, we investigate the effect of aqueous solution-processed V_2O_5 (labelled V_2O_5–w) on the stability of polymer:fullerene bulk heterojunction solar cells and compare its performance with PEDOT:PSS. This water-based V_2O_5 oxide is highly compatible with the fabrication of thin film solar cells by large-area, low-cost, fast processing, and high-throughput printing fabrication.[14,17] Lab-scale OPVs on glass fabricated by spin

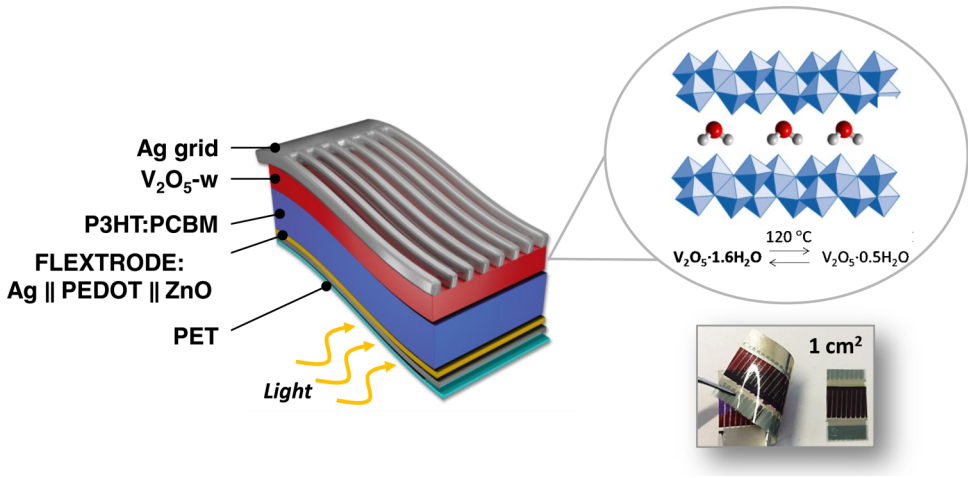

FIG. 1. Schematic representation of the organic solar cell configuration (left) and the structure of the water-based V_2O_5 hole transport layer (right).

coating applying the V_2O_5–w have already been fabricated in our group and demonstrated outdoor stability for more than 1000 h.[21] Here we demonstrate the fabrication of flexible ITO-free OPVs applying the V_2O_5–w fabricated by slot-die roll-coater. We will show the outdoor stability analyses of the flexible ITO-free OPVs for more than 900 h and demonstrate that the application of the oxide results in greater stability if compared to devices applying PEDOT:PSS.

We prepared inverted OPV devices with the configuration PET/Ag/PEDOT/ZnO/P3HT:PC_{60}BM/HTL/Ag (Fig. 1). The hole transport layer (HTL) was the V_2O_5–w and PEDOT:PSS, and the latter was used for comparison purposes. The water-based V_2O_5 was synthesised by the sol-gel method as reported.[21] The active layer for the single junction device was composed of P3HT (electronic grade from Rieke) and PC_{60}BM (technical grade from Solenne BV). The PEDOT:PSS Clevios SV3 was brought from Heraeus. The V_2O_5 was diluted with isopropyl alcohol in the ratio 1:2 (w/w), and the PEDOT:PSS was diluted to a viscosity of 300 mPa s. A highly conductive PEDOT:PSS (Clevios PH1000 from Heraeus) was used to improve the contact between the HTL and the back electrode (Ag). This PEDOT:PSS was diluted with isopropyl alcohol in the ratio 10:3 (w/w), and its sheet resistivity was 60 Ω $Square^{-1}$. The back silver grid was printed using a screen printing silver past (PV410 from Dupont). Coating was performed on Flextrode that comprises a highly conducting metal grid, semi-transparent conductor, and hole blocking layer (PET/Ag/PEDOT/ZnO). The Flextrode was mounted on the roller using heat stable tape (3M) and the procedure began by first slot-die coating the active layer consisting of P3HT:PCBM (1:1, by weight) dissolved in chlorobenzene (40 mg/ml), with an addition of 10% of chloroform and 3% of chloronaphthalene. It was printed on the Flextrode electrode at 0.1 ml/min flow and 1.3 m/min for the web at 70 °C. The PEDOT:PSS layer was slot-die coated at 80 °C with a web speed 0.5 m/min. The V_2O_5 layer was slot-die coated at 90 °C with a web speed of 1.0 m/min. The flow of the solution was varied to give different thicknesses; the applied flows were 0.20 ml/min, 0.15 ml/min, and 0.10 ml/min. The theoretical, dry thickness for these layers is 80, 60, and 40 nm, respectively. The highly conductive PEDOT:PSS was slot-die coated on top of the HTL at 70 °C with a web speed of 0.4 m/min. The back silver electrode was applied by flexographic printing of heat curing silver paste PV410 (Dupont). The silver paste was added to the flexographic roll and further transferred to the substrate with a web speed of 1.2 m/min and roll temperature of 80 °C. The outdoor stability analyses were made following the ISOS-O-2 procedure[27] at the Catalan Institute of Nanoscience and Nanotechnology (ICN2-CSIC), located in Barcelona, Spain (41.30° N, 2.09° W), using a solar tracking positioning system. The system comprises a large dual axis-controlled platform with fully automated motors, which enables turning of the tracker hour angle up to 100° (which translates to nearly 7 h of perpendicular solar tracking) and turning of the tracker elevation angle from 15° to 90° (which enables full tracking of solar elevation). We developed in-house software to control

the photovoltaic response of sixteen solar cells at the same time and to continuously monitor light irradiation, temperature, and relative humidity over time. IV-curves were measured using a 2602 A dual-channel SMU multimeter and a 3700 series switch/multimeter (both from Keithley). PCE values were calculated using the maximum daily irradiance level. The light irradiation was measured with a Zipp & Konen CM-4 pyranometer. The temperature and relative humidity were monitored with a combined sensor (Theodor Friedrichs). Analyses were made in the summer of 2014, between the months of June and September.

V_2O_5 HTLs have been synthesised chiefly by multistep techniques.[21] As already mentioned, the applied fabrication methods are those obtained from sol–gels made from vanadium (V) oxytriisopropoxide (ViPr) or $(NH_4)_3VO_4$, among others.[14–20] In these cases, the precursor materials are selected for the fabrication of flexible solar cells where the sintering temperatures cannot exceed 150 °C. Nevertheless, some organic residues from the precursors are not eliminated at those temperatures and are usually observed after thin film coating. In other cases, the precursors are not completely transformed into the oxide compound at low temperatures (see Fig. S1 in the supplementary material[28]). The V_2O_5 applied in this work is already an oxide at room temperature; it is in the form of a gel after synthesis and presents a layered crystalline structure where water molecules are intercalated between the oxide slabs (Fig. 1). There are no residues other than water after the V_2O_5–w is coated and heated at 120 °C, and the water molecules can be easily eliminated with soft heat. The latter makes this material very suitable for low temperature deposition by printing methods on flexible substrates (e.g., PET). The as-prepared thin film heated at 120 °C presents a nanostructured topology (Figs. 2(a) and 2(b)) and a preferential orientation of the layer structure as observed by gracing incidence X-ray diffraction analyses (Fig. 2(c)). While a powder sample will display crystalline peaks corresponding to the V_2O_5 oxide samples, a coated film shows the preferential orientation of the microcrystalline thin film at the C-axis, or perpendicular to the film plane. These peaks can be indexed as the $V_2O_5{\cdot}H_2O$ monoclinic phase in well agreement with

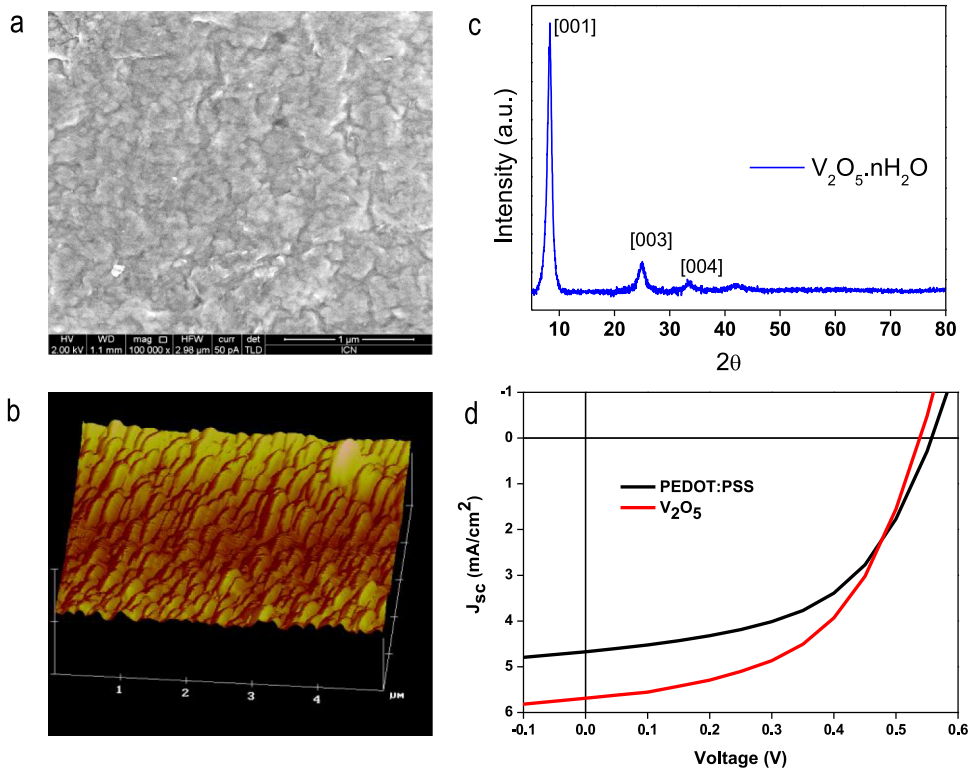

FIG. 2. Thin film of water based V_2O_5: (a) SEM top image, (b) AFM topography, (c) gracing incidence X-ray diffraction analysis, and (d) IV-curve of an inverted organic solar cell with the configuration PET/Ag/PEDOT/ZnO/P3HT:PC_{60}BM/HTL/Ag applying V_2O_5 and PEDOT:PSS as the HTL.

TABLE I. Average of five ITO-free OPVs with inverted configuration applying V_2O_5 and PEDOT:PSS as the HTLs. Data obtained under a sun simulator at 1000 mW/cm^2.

HTL	J_{SC} (mA cm^2)	V_{OC} (V)	*FF*/(%)	η (%)	η (*max*)/%
PEDOT:PSS	4.48 ± 0.22	0.56 ± 0.01	51.29 ± 0.66	1.27 ± 0.07	1.36
V_2O_5	5.18 ± 0.40	0.54 ± 0.00	53.29 ± 1.61	1.49 ± 0.07	1.59

pattern (JCPDS 21-1432).[26] The intensity of the (001) peak is assumed to be proportional to the fraction of quasi-ordered crystalline material in the sample, and usually, this peak is observed to increase as the annealing temperature increases. The interlayer spacing *d* in the $V_2O_5{\cdot}n\ H_2O$ structure was calculated from the (001) diffraction peak at 2θ = 8.24°, resulting in a 10.76 Å. This value corresponds to one monolayer of water molecules intercalated within the V_2O_5 slabs, as expected.

We prepared inverted ITO-free OPV devices on PET, and the PCE of the device with V_2O_5 showed higher PCE than devices applying PEDOT:PSS hole transport layer (Table I, Figure 2(d)). The average of five devices analysed for each HTL with active area of 1 cm^2 is shown in Table I. The values of voltage (Voc) and fill factor (FF) are almost identical, 0.56 V and 0.54 V and 51% and 53% for PEDOT:PSS and V_2O_5, respectively. Major changes are observed for J_{sc}, which is larger for the OPV applying the water, based on V_2O_5.

The lifetime of OPVs is dependent on factors such as oxygen and moisture, especially when the PEDOT:PSS is applied due to its hygroscopic nature.[22,23] Due to the high relative humidity of the location of our outdoor testing facility (80% RH in Barcelona, Spain), the solar cells were encapsulated in glass for stability tests. Sealing our devices in glass permits to eliminate variables such as any defects from the encapsulation (any permeation issues, pinholes, or similar from the PET substrate) which is not the aim of our work. Fig. 3 shows the outcome of the outdoor stability test performed for the first 900 h to the OPVs applying the PEDOT:PSS (Fig. 3(a)) and the water-based V_2O_5 (Fig. 3(b), Table II). Values of irradiance (between 850 and 1000 mW/cm^2) and temperature (°C) are also included in each graph.

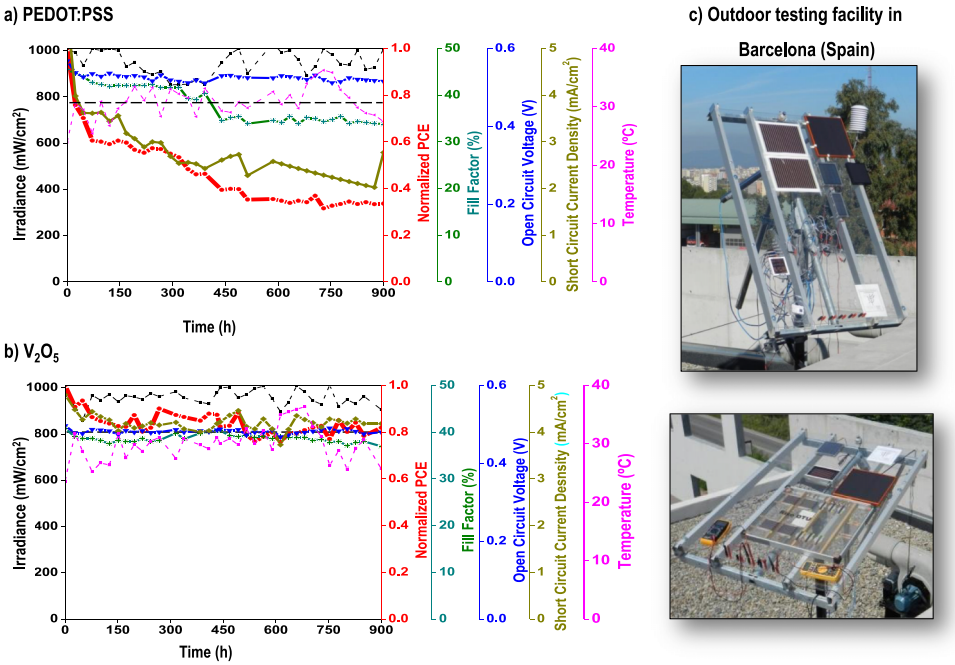

FIG. 3. Outdoor stability analyses (ISOS-O-2) of flexible OPV with an inverted configuration of the type PET/Ag/PEDOT/ZnO/P3HT:$PC_{60}BM$/HTL/Ag, where the HTL is PEDOT:PSS (a) or our water-based V_2O_5 (b). Active area is 1 cm^2. Outdoor analyses carried out at the outdoor testing facility of ICN2 in Barcelona, Spain (c). Data points correspond to sunlight irradiation between 850 and 1000 mW/cm^2 and temperature was measured to be below 35 °C.

TABLE II. Photovoltaic parameters evolution of the outdoor stability analysis of an inverted configuration OPV of the type PET/Ag/PEDOT/ZnO/P3HT:$PC_{60}BM$/HTL/Ag, where the HTL is our water-based V_2O_5 or PEDOT:PSS. Data obtained for the irradiation between 850 and 1000 mW/cm^2 in the outdoor sun tracker system in Barcelona, Spain.

PEDOT:PSS time (h)	J_{SC} (mA/cm^2)	V_{OC} (V)	*FF*/(%)	η (%)	X in T_x[a]
Initial	4.19	0.54	45.48	1.20	0
300 h	3.05	0.53	42.31	0.79	66
600 h	2.22	0.52	34.64	0.46	40
900 h	1.95	0.51	38.28	0.47	40
V_2O_5–wt time (h)	J_{SC} (mA/cm^2)	V_{OC} (V)	*FF*/(%)	η (%)	X in T_x
Initial	4.55	0.48	39.79	1.06	0
300 h	4.05	0.48	37.28	0.81	80
600 h	3.80	0.48	38.92	0.84	82
900 h	4.02	0.48	37.87	0.83	82

[a]x in Tx is defined as the point at which the efficiency of the device reaches X% of the initial efficiency.

The first interesting feature is that although the V_2O_5 layer has water molecules intercalated within its crystalline structure, the stability response of the device is steady and superior than the one observed for OPVs applying the PEDOT:PSS (Fig. 3). The observed T_{80} lifetime (defined as the point at which the efficiency of the device reaches 80% of the initial efficiency, see Table II) was observed after only a few hours for PEDOT:PSS and after 400 h for the V_2O_5 (Fig. 3(b) and Table II). The period of time before reaching T_{80} is a well-known event for OPVs related to the "burn-in" process that is characterized by an initial sudden drop in PCE followed by a stabilization of the solar cell response.[24] For devices applying the PEDOT:PSS OPV (Fig. 3(b) and Table II), the Voc and FF are maintained almost unchanged during the first 800 h, while Jsc and PCE show the aforementioned "burn-in" process and a drastic drop in efficiency until 400 h. In the case of devices with V_2O_5, the Voc and FF were kept almost unaffected for the whole stability analyses, and efficiency and Jsc were observed to drop only after 400 h. For the devices applying the PEDOT:PSS HTL, 40% of the initial PCE was maintained at the end of the test, after 900 h, while the OPV applying the V_2O_5 layer maintained the initial PCE at around 80% of the initial value after the same period of time.

The evolution of the IV curves throughout the stability tests for each of the OPVs is show in Fig. 4. In both types of OPVs, the V_{oc} is kept almost identical after the degradation test, an indication that the interface between the active layer and the electrodes (HTL or ETL) is almost unaffected in both devices. The changes observed in FF are the result of different causes, among them is the reduced interfacial charge transfer efficiency between the different layers, the degradation of the active layer, or the increase of the recombination processes. These processes can be taking place in both OPVs but in the case of the devices applying the PEDOT:PSS, the drop in FF is stronger, especially at the end of the stability analysis. The strongest changes are observed on Jsc and, as a consequence, on the PCE. Changes in Jsc are due to many internal processes inside the OPV, like the increase of internal resistance due to the degradation of the electron transport layers, the electron donor, or due to the reduction of the transparency of any layer or interface, which could reduce the amount of light entering the cell. In general, all these degradation processes are taking place much faster and stronger for OPV devices applying the PEDOT:PSS HTL demonstrating the beneficial effect of applying the aqueous-processed V_2O_5–w HTL.

The beneficial effect on stability when our V_2O_5 oxide HTL is applied is clearly demonstrated with these results. Moreover, the feasibility to synthesise the gel in its oxide form at room temperature (Fig. 2) is also an advantage if compared to other oxides where the precursors are not completely transformed into the oxide at low temperatures. This is the case of the synthesis of V_2O_5 from precursors like powder V_2O_5 and $(NH_4)_3VO_4$.[12] Long *et al.* reported the fabrication of OPVs by employing this precursor for the preparation of the oxide layer as charge injection.[25] The authors demonstrated a similar power conversion efficiency of the OPV if compared with PEDOT:PSS but no stability test was carried out. Our X-ray diffraction analyses of a thin film made with this precursor showed that the $(NH_4)_3VO_4$ is transformed into the oxide until heating at 350 °C

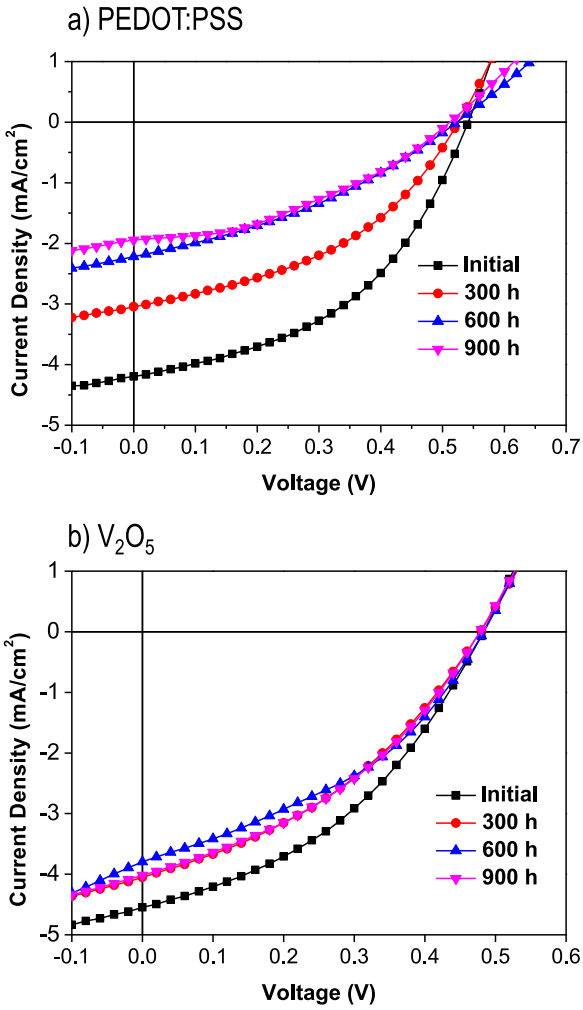

FIG. 4. Evolution of the IV curves throughout the outdoor stability analyses for 900 h (ISOS-O-2) of inverted configuration OPV of the type PET/Ag/PEDOT/ZnO/P3HT:PC_{60}BM/HTL/Ag, where the HTL is (a) PEDOT:PSS or (b) our water-based V_2O_5.

(Fig. S1).[28] Although the PCE of the device shows the same PCE (see Figure S2 and Table S1 in the supplementary material[28]), the stability of the solar cell is even worse than the one observed for OPVs applying PEDOT:PSS (Fig. S3).[28]

In summary, we have analysed the stability of flexible ITO-free organic solar cells fabricated by slot-die roll-to-roll methods applying a water-based V_2O_5 hole transport layer. The devices of 1 cm^2 active area were compared to OPVs applying PEDOT:PSS. Outdoor stability analysis (ISOS-O-2) revealed that, although the V_2O_5 contain water molecules within its structure, the device stability surpass greatly the stability of OPV devices fabricated with PEDOT:PSS.

ICN2 acknowledges the support of the Spanish MINECO through the Severo Ochoa Centers of Excellence Program under Grant Nos. SEV-2013-0295 and ENE2013-48816-C5-4-R. Thanks goes to the Agència de Gestió d'Ajuts Universitaris i de Recerca for the support through the Xarxa de Referència en Materials Avançats per a l'Energia (XaRMAE) and the consolidated research group No. 2014SGR-1212. To the COST Action StableNextSol Project No. MP1307. To CNPq and FUNCAP (Brazil) for the financial support to A.L., A.B., and I.V. Thanks goes to the European Research Infrastructure (SOPHIA) (Grant No. 262533) for providing access to manufacturing equipment at DTU. This work is being carried out under the Materials Science Ph.D. degree for Y.R. of the Universitat Autònoma de Barcelona.

[1] W. J. Yu, L. Shen, S. P. Ruan, F. X. Meng, J. L. Wang, E. R. Zhang, and W. Y. Chen, Sol. Energy Mater. Sol. Cells **98**, 212–215 (2012).
[2] J. Jung, D. Kim, W. S. Shin, S. J. Moon, C. Lee, and S. C. Yoon, Jpn. J. Appl. Phys., Part 1 **49**(5), 05EB05 (2010).
[3] A. K. K. Kyaw, X. W. Sun, C. Y. Jiang, G. Q. Lo, D. W. Zhao, and D. L. Kwong, Appl. Phys. Lett. **93**(22), 221107 (2008).
[4] S. Han, W. S. Shin, M. Seo, D. Gupta, S. J. Moon, and S. Yoo, Org. Electron. **10**(5), 791–797 (2009).
[5] K. Takanezawa, K. Tajima, and K. Hashimoto, Appl. Phys. Lett. **93**(6), 063308 (2008).
[6] J. Kim, G. Kim, T. K. Kim, S. Kwon, H. Back, J. Lee, S. Ho Lee, H. Kang, and K. Lee, J. Mater. Chem. A **2**, 17291–17296 (2014).
[7] C. Chueh, C. Li, and A. K.-Y. Jen, Energy Environ. Sci. **8**, 1160-1189 (2015).
[8] J. W. Jung, C. Chueh, and A. K.-Y. Jen, Adv. Mater. **5**, 1500486 (2015).
[9] Y. H. Lin, P. C. Yang, J. S. Huang, G. D. Huang, I. J. Wang, W. H. Wu, M. Y. Lin, W. F. Su, and C. F. Lin, Sol. Energy Mater. Sol. Cells **95**(8), 2511–2515 (2011).
[10] S. R. Hammond, J. Meyer, N. E. Widjonarko, P. F. Ndione, A. K. Sigdel, A. Garcia, A. Miedaner, M. T. Lloyd, A. Kahn, D. S. Ginley, J. J. Berry, and D. C. Olson, J. Mater. Chem. **22**(7), 3249–3254 (2012).
[11] K. Zilberberg, H. Gharbi, A. Behrendt, S. Trost, and T. Riedl, ACS Appl. Mater. Interfaces **4**(3), 1164–1168 (2012).
[12] M. Y. Lin, C. Y. Lee, S. C. Shiu, I. J. Wang, J. Y. Sun, W. H. Wu, Y. H. Lin, J. S. Huang, and C. F. Lin, Org. Electron. **11**(11), 1828–1834 (2010).
[13] Y. M. Chang and J. M. Ding, Thin Solid Films **520**(16), 5400–5404 (2012).
[14] K. Zilberberg, S. Trost, J. Meyer, A. Kahn, A. Behrendt, D. Lützenkirchen-Hecht, R. Frahm, and T. Riedl, Adv. Funct. Mater. **21**(24), 4776–4783 (2011).
[15] C. P. Chen, Y. D. Chen, and S. C. Chuang, Adv. Mater. **23**(33), 3859–3863 (2011).
[16] I. Hancox, L. A. Rochford, D. Clare, M. Walker, J. J. Mudd, P. Sullivan, S. Schumann, C. F. McConville, and T. S. Jones, J. Phys. Chem. C **117**(1), 49–57 (2013).
[17] T. T. Larsen-Olsen, T. R. Andersen, B. Andreasen, A. P. L. Böttiger, E. Bundgaard, K. Norrman, J. W. Andreasen, M. Jørgensen, and F. C. Krebs, Sol. Energy Mater. Sol. Cells **97**, 43-49 (2012).
[18] K. Zilberberg, S. Trost, H. Schmidt, and T. Riedl, Adv. Energy Mater. **1**(3), 377–381 (2011).
[19] J. Livage, Coord. Chem. Rev. **190-192**, 391–403 (1999).
[20] Q. Yue, H. Jiang, Y. Hu, G. Jia, and C. Li, Chem. Commun. **50**, 13362–13365 (2014).
[21] G. Terán-Escobar, J. Pampel, J. M. Caicedo, and M. Lira-Cantú, Energy Environ. Sci. **6**(10), 3088–3098 (2013).
[22] A. M. Nardes, M. Kemerink, M. M. de Kok, E. Vinken, K. Maturova, and R. A. J. Janssen, Org. Electron. **9**(5), 727–734 (2008).
[23] T. S. Glen, N. W. Scarratt, H. Yi, A. Iraqi, T. Wang, J. Kingsley, A. R. Buckley, D. G. Lidzey, and A. M. Donald, Sol. Energy Mater. Sol. Cells **140**, 25–32 (2015).
[24] R. Roesch, T. Faber, E. von Hauff, T. M. Brown, M. Lira-Cantu, and H. Hoppe, Adv. Energy Mater. **5**, 1501407 (2015).
[25] D. X. Long, Y. Xu, S. Kang, W. Park, E. Choi, Y. Nah, C. Liu, and Y. Noh, Org. Electron. **17**, 66–76 (2015).
[26] V. Petkov, P. N. Trikalitis, E. S. Bozin, S. J. L. Billinge, T. Vogt, and M. G. Kanatzidis, J. Am. Chem. Soc. **124**(34), 10157–10162 (2002).
[27] M. O. Resee *et al.*, Sol. Energy Mater. Sol. Cells **95**(5), 1253–1267 (2011).
[28] See supplementary material at http://dx.doi.org/10.1063/1.4942638 for the photovoltaic response of OPVs applying a transparent V_2O_5 hole transport layer.